Projectile coherence effects in electron capture by protons colliding with H_2 and He

S. Sharma,[1] A. Hasan,[1,2] K. N. Egodapitiya,[1,*] T. P. Arthanayaka,[1] G. Sakhelashvili,[1,3] and M. Schulz[1,†]

[1]*Department of Physics and LAMOR, Missouri University of Science & Technology, Rolla, Missouri 65409, USA*

[2]*Department of Physics, UAE University, P. O. Box 17551, Alain, Abu Dhabi, United Arab Emirates*

[3]*College of Arts and Sciences, Ilia State University, 0162 Tblisi, Georgia*

(Received 14 May 2012; published 8 August 2012)

We have measured differential cross sections for single and dissociative capture for 25 and 75 keV protons colliding with H_2 and He. Significant differences were found depending on whether the projectile beam was coherent or incoherent. For 75 keV $p + H_2$ these differences can be mostly associated with molecular two-center interference and possibly some contributions from path interference. For 25 keV (both targets) they are mostly due to path interference between different impact parameters leading to the same scattering angles and, for the H_2 target, possibly some contributions from molecular two-center interference.

DOI: 10.1103/PhysRevA.86.022706 PACS number(s): 34.70.+e

I. INTRODUCTION

To accurately calculate atomic scattering cross sections remains a very challenging task even after several decades of research. The basic underlying difficulty is that the Schrödinger equation is not analytically solvable for more than two mutually interacting particles. Therefore, elaborate numerical methods have been developed and reliable theoretical total cross sections are routinely obtained for a broad range of collision systems and for a variety of processes (for reviews see, e.g., [1,2]). In the case of ionization, differential ejected electron spectra can also be reproduced by theory with remarkable accuracy even at very large perturbation (projectile charge to speed ratio η) [3], which is considered to be a particularly challenging regime.

These successes sharply contrast with serious problems which arise when experimental and theoretical data are compared for cross sections differential in projectile parameters. For the same collision system for which measured differential electron spectra are nicely reproduced by theory (3.6 MeV/amu $Au^{53+} + He$, $\eta = 4.5$ [3]), severe discrepancies are observed in the double differential cross sections (DDCSs) as a function of electron energy and projectile momentum transfer q [4]. In fully differential cross sections (FDCSs) significant discrepancies were even observed for very small η (0.1) [5], for which the collision dynamics was thought to be essentially understood. The disagreement with experiment was particularly pronounced in fully quantum-mechanical calculations [e.g., [5–8]], but surprisingly, if the interaction between the projectile and the target core (PT interaction) was treated classically or semiclassically, good or at least improved agreement was achieved [9–12].

Numerous attempts have been made to explain these discrepancies. Fiol *et al*. [8] attributed them entirely to the experimental resolution. However, a more thorough analysis, based on more realistic parameters, revealed that the resolution can account for only a small fraction of the discrepancies [9,13]. Madison *et al*. [14] have pointed out that in their distorted-wave approach the three-body final-state wave function may not be accurate if all particles are close together. On the other hand, a nonperturbative approach, which is not affected by this problem, yielded essentially the same results [15]. Foster *et al*. [16] observed that for electron impact the calculations were very sensitive to the description of the screening of the target nucleus by the passive electron, but for ion impact at small η Voitkiv and Najjari [7] did not find a significant change with varying screening. Finally, one might expect that the presence of the second electron in the target atom could have a noticeable effect on the cross sections beyond merely screening the nucleus. For example, correlation between the two electrons could be important, or other reaction channels (like, e.g., ionization plus excitation), not present for a one-electron target, could be stronger than expected. However, in recent experiments significant discrepancies between theory and experiment were found in the DDCSs even for an atomic hydrogen target [17].

The key to resolving the puzzling discrepancies between theory and experiment, even for small η, was provided by new experimental developments. Earlier, path interference and molecular two-center interference of a single electron ejected in atomic collisions was predicted by theory [e.g., [18] and experimentally observed [e.g., [19–21]. More recently we demonstrated that in the scattering angle dependence of the DDCS for ionization in $p + H_2$ collisions an interference pattern, due to indistinguishable diffraction of the projectiles from the two atomic centers of the molecule, was present for a coherent but not for an incoherent projectile beam [22]. In analogy to classical optics the transverse coherence length Δr is determined by the geometry of a collimating slit placed before the target and the de Broglie wavelength of the projectile wave λ by [23]

$$\Delta r = (1/2)(L/a)\lambda, \tag{1}$$

where a and L are the width of the collimating slit and its distance from the target. In optical Young double-slit interference the requirement for transverse coherence is that Δr is larger than the double-slit separation. In the case of ionization of H_2 the role of the slit separation is taken by the

*Present address: Dept. of Physics, University of Virginia, 382 McCormick Rd, Charlottesville, VA 22904-4714.

†schulz@mst.edu

internuclear distance D in the molecule. The experiment of Ref. [22] was performed for two different L corresponding to $\Delta r = 3$ and 0.4 a.u., respectively. With $D = 1.4$ a.u., the projectile beam was coherent for the larger and incoherent for the smaller value of Δr.

Furthermore, we proposed in [22] that the discrepancies between experiment and theory in the FDCS for ionization of He could be due to artificial path interference in the calculations. Consider, for example, the first-order amplitude, where the projectile gets deflected only from the target electron, and a second-order amplitude involving the PT interaction so that the projectile is deflected attractively (by the electron) and repulsively (by the nucleus). One would expect that for these two amplitudes different impact parameter ranges mainly contribute to the same scattering angle θ [24]. In the calculations, the coherent sum of both leads to an interference term. Indeed, this type of interference was recently found in perturbative calculations of FDCSs for intermediate-energy $p + \mathrm{He}$ collisions [25]. However, an observable interference requires a coherent projectile beam. On the other hand, Δr realized in the experiments is typically very small compared to atomic dimensions, especially for small η, and the interference term is then not observable. Recently, FDCS measurements were performed for small η at an ion storage ring, where coherent projectile beams can be prepared through electron cooling [26]. Indeed, in this study the discrepancies between experiment and theory observed for an incoherent beam are largely resolved.

The important role of the projectile coherence has been overlooked for decades of atomic collision studies and is still largely unexplored. The recent findings just represent the beginning of a new research direction in this field. A systematic study of the role of the projectile coherence, extending the initial measurements to a broad range of collision systems and scattering processes, is necessary to gain a complete understanding of interference phenomena in atomic collisions. In this article, we report results of such studies on electron capture in collisions of protons with He and H_2 which confirm the important role of the projectile coherence.

II. EXPERIMENT

A sketch of the experimental setup is shown in Fig. 1. A proton beam was generated with a hot-cathode ion source and accelerated to energies of 25 and 75 keV. A pair of collimating slits, each with a width of 0.15 mm, was placed in front of the target region at a distance $L_x = 6.5$ cm in the x direction and $L_y = 50$ cm in the y direction. The beam intersected with a very cold ($T \approx 2$ K) H_2 or He beam from a supersonic jet. After the collision, the projectiles were charge-state analyzed by a switching magnet and the neutralized beam component hit a two-dimensional position-sensitive channel-plate detector. From the position information we obtained θ.

The direct proton beam, deflected in the switching magnet, was energy analyzed, with the target gas taken out, using an electrostatic parallel-plate analyzer [27]. The measured energy distribution had a width of ± 0.5 eV, which is mostly due to the resolution of the energy analyzer. The energy spread in the beam is significantly smaller. The width of the angular

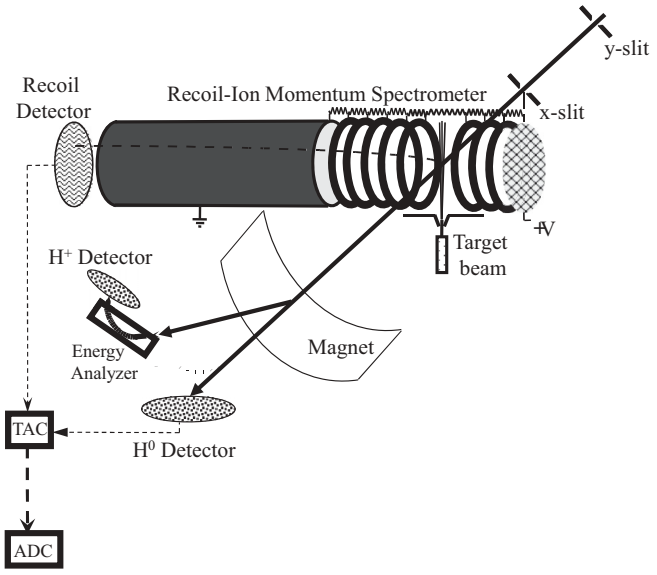

FIG. 1. Schematic diagram of the experimental setup. TAC represents a time-to-amplitude converter and ADC an analog-to-digital converter.

distribution of the direct beam was measured to be about ± 75 μrad.

The recoiling H_2^+ and He^+ ions were extracted by a weak electric field ($\approx$4.5 V/cm), directed perpendicular to the projectile beam direction, and also detected by a two-dimensional position-sensitive detector. For the smaller collision energy (25 keV) we also obtained data for molecular proton fragments, produced in dissociative capture, extracting them with a field of about 35 V/cm. The recoil-ion detector and the neutralized projectile detector were set in coincidence. From the time-of-flight information (contained in the coincidence time spectrum) the recoil-ion momentum component in the direction of the extraction field (x direction) was calculated and from the position information the component parallel to the projectile beam (z direction) and the y component were calculated. Since capture is a two-body scattering process, the recoil-ion momentum is equal to the momentum transfer $\mathbf{q}$ from the projectile to the target. For the H_2^+ and He^+ ions the momentum resolution in the y direction (mostly due to the temperature of the target beam) was approximately ± 0.25 a.u. and in the x and z directions ± 0.075 a.u. In the case of the molecular proton fragments the momentum resolution was much worse (approx. ± 0.6 a.u. in all directions) due to the much larger extraction field so that here $\mathbf{q}$ could not be determined with sufficient accuracy from the recoil ions.

Due to the different distances of the collimating slits in the x and y directions the coherence length of the projectile is different in both directions. According to Eq. (1) in the x direction it is $\Delta x = 0.4$ and 0.7 a.u. for projectile energies of 75 and 25 keV, respectively, while for the y direction these values are $\Delta y = 3$ and 5 a.u. so that for both energies $\Delta x < D$ and $\Delta y > D$. Therefore, by selecting projectile scattering in the x and y directions in the position spectrum, we obtain the differential cross sections (DCSs) as a function of scattering angle for a coherent and incoherent projectile beam simultaneously in the same data run.

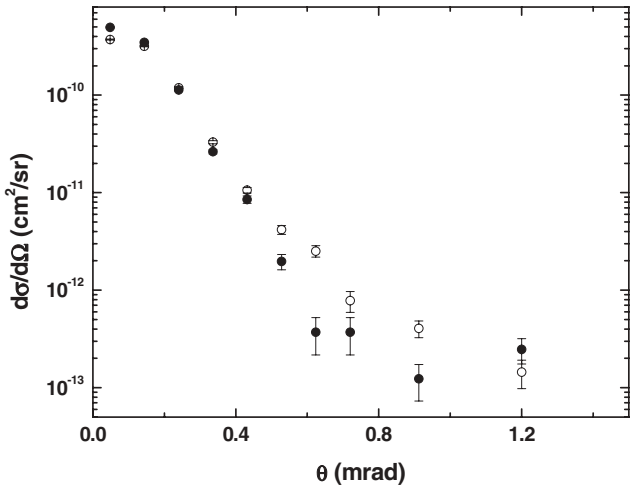

FIG. 2. Differential cross sections as a function of scattering angle for nondissociative capture in 75 keV $p + H_2$ collisions. The open symbols represent the data taken at the small slit distance (i.e., for an incoherent projectile beam) and the closed symbols data taken at the large slit distance (i.e., for a coherent projectile beam).

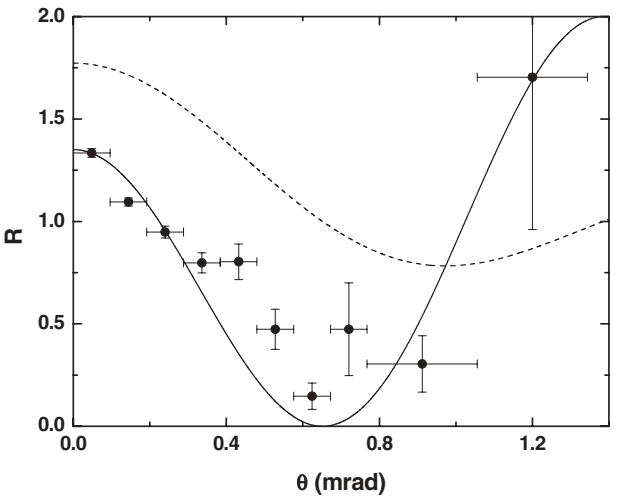

FIG. 3. Differential ratios between the cross sections for a coherent and an incoherent projectile beam as a function of scattering angle for 75 keV $p + H_2$. Solid curve, calculation based on Eq. (2) assuming a molecular orientation along **q**; dashed curve, calculation based on Eq. (3).

III. RESULTS AND DISCUSSION

Since capture is kinematically a two-body scattering process the momentum analysis of one particle already constitutes a kinematically complete experiment. Therefore, for an ideal experiment, i.e., one with infinitely good resolution and no background, measuring the recoil-ion momentum in addition to the projectile momentum would not provide any additional information. However, in reality background cannot be completely avoided (and the resolution is, of course, limited). For example, the projectile position spectrum could potentially be affected by scattering from the collimating slits. If such a slit-scattered projectile subsequently undergoes a capture process with the target this can still lead to a true coincidence. However, the scattering angle deduced from the projectile position spectrum would not be correct, while the scattering angle deduced from the recoil-ion momentum would essentially not be affected by slit scattering. Likewise, background contributions to the recoil-ion spectra, for example due to the small (but nonzero) diffusive target gas component, do not significantly affect the projectile spectra. Therefore, the overdetermination of the kinematics due to the momentum-analyzed detection of both particles can be used to clean such background contributions from the data. This was achieved with the condition that θ determined from the projectiles directly and θ determined from the recoil ions must be equal within ± 0.1 mrad.

In Fig. 2 we show the DCSs for nondissociative capture in 75 keV $p + H_2$ collisions as a function of θ for the coherent (closed symbols) and the incoherent (open symbols) projectile beams. Once again, as in the corresponding DDCSs for ionization in the same collision system [22], clear differences between the two data sets are visible. At $\theta = 0$ the coherent cross sections (DCS_{coh}) are slightly larger than the incoherent data (DCS_{inc}) before the two data sets cross around 0.2 mrad; with increasing θ the DCS_{coh} then increasingly drop below DCS_{inc} up to about $\theta = 0.8$ mrad, and both data sets seem to approach each other again with further increasing θ (although this trend at large θ is statistically not conclusive). Qualitatively, this is the same behavior as in ionization.

In analogy to classical optics the interference term (I) is given by the ratio R between DCS_{coh} and DCS_{inc} [22,28], which is plotted in Fig. 3 as a function of θ. It should be noted that at $\theta = 0$ the x and y directions are not defined. Here, the pixels in the two-dimensional xy position spectrum containing the events for both directions are identical so that the ratio between the un-normalized count rates is equal to unity and does not reflect the I. Since the first data point ($\theta = 0.05$ mrad) covers the bin 0 to 0.1 mrad it is partly affected. The DCS_{coh} and DCS_{inc} shown in Fig. 2 are normalized to the same total cross section [29] resulting in R differing from 1 at $\theta = 0.05$ mrad. Apart from this artifact near $\theta = 0$, once again the data look similar to the corresponding ratios for ionization.

For a fixed molecular orientation I can be expressed as

$$I = 1 + \cos(\boldsymbol{p}_{rec} \cdot \boldsymbol{D}) = 1 + \cos(\boldsymbol{q} \cdot \boldsymbol{D}). \quad (2)$$

In our experiment the molecular orientation was not measured and therefore I has to be integrated over all orientations. If the angular distribution of the molecules during the capture process is isotropic this integral yields [28]

$$I = 1 + \sin(qD)/(qD). \quad (3)$$

On the other hand, it is not clear that all orientations are uniformly distributed. For example, in ionization of H_2 by electron impact Senftleben *et al.* [30] found a preference of the molecules to be oriented along **q**. The solid line in Fig. 3 shows I calculated with Eq. (2) replacing $\mathbf{q}\cdot\mathbf{D}$ by qD, i.e., assuming that the molecule is always oriented along **q**, and the dashed curve I calculated with Eq. (3). The curves do not reach $I = 2$ at $\theta = 0$ because q is not zero due to the θ-independent longitudinal component $q_z = \Delta E/v - v/2$ (where ΔE and v are the energy loss and the speed of the projectile). The experimental data fall, crudely speaking, in between both

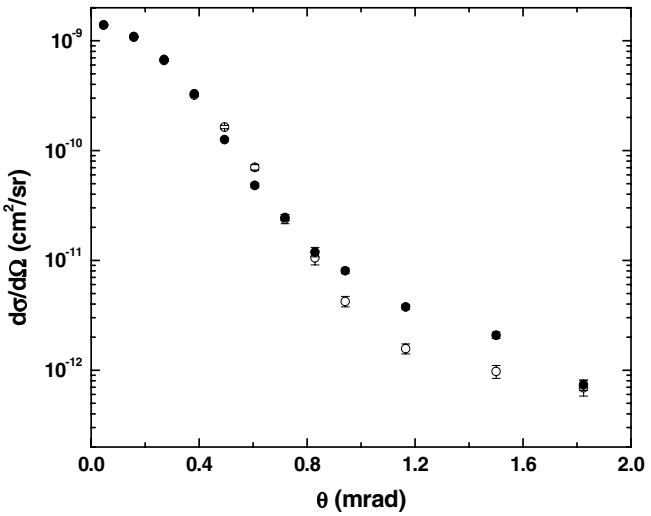

FIG. 4. Same as Fig. 2 for 25 keV $p + H_2$.

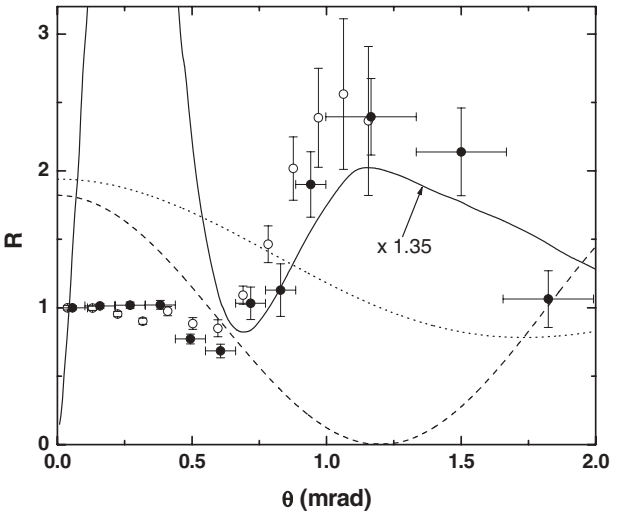

FIG. 5. Same as Fig. 3 for 25 keV $p + H_2$ (closed symbols) and 25 keV $p + He$ (open symbols). Dashed curve, calculation based on Eq. (2) assuming a molecular orientation along **q**; dotted curve, calculation based on Eq. (3); solid curve, ratio between calculations treating the PT interaction quantum-mechanically and classically, respectively [31] (see text).

calculations, which is consistent with a preferential, but not exclusive, orientation along **q**.

It should be noted that it is actually the component of **D** perpendicular to the projectile beam axis, $D_\perp$, which matters in the coherence requirement, which should thus read $\Delta r > D_\perp$. If the molecule is indeed preferentially oriented along **q** this means that even in the x direction the projectile beam becomes coherent below some critical θ because **q** (and therefore the molecular orientation) is increasingly aligned along the beam axis with decreasing θ. However, for 75 keV this happens only at $\theta \approx 70$ μrad (corresponding to a molecular orientation of about 15° relative to the beam axis) so that at most the data point at the smallest θ is affected.

In Fig. 4 the DCS_{coh} (closed symbols) and DCS_{inc} (open symbols) are shown as functions of θ for 25 keV $p + H_2$. Here too, there are some differences between both data sets. However, the comparison between DCS_{coh} and DCS_{inc} is qualitatively different from the 75 keV case. This is more apparent in the ratios R, which are plotted in Fig. 5 as functions of θ. For $\theta < 0.8$ mrad R is nearly constant at 1 with only a small minimum around 0.5 mrad. At large θ there is a pronounced and broad maximum near 1.2 mrad. This θ dependence does not resemble either the interference term calculated with Eq. (2) (dashed curve in Fig. 5), assuming a molecular orientation along **q**, or the one calculated with Eq. (3) (dotted curve). The flat region in the experimental data, not reproduced by either calculation, could possibly be associated to some extent with the coherence requirement $\Delta r > D_\perp$ being satisfied even in the x direction (small slit distance) at small θ (see above). For 25 keV this can happen already at about 0.15 mrad (where $\Delta x = D_\perp$, again assuming that the molecule is preferentially oriented along **q**) because Δx is larger than at 75 keV due to the larger de Broglie wavelength. However, this would explain only part of the flat region, which extends to at least 0.4 mrad. More importantly, this would not explain the maximum at large θ not reproduced by Eq. (2) or (3), which predict a minimum, rather than a maximum, in this region. The data thus seem to suggest that molecular two-center interference is either not present at 25 keV or it is at least not the dominant interference effect.

For capture processes at small projectile energies interference structures have been observed in the calculated θ dependence of the DCS even for atomic targets [31,32] which are thus not due to molecular two-center interference. Furthermore, it was found that this structure disappears if the PT interaction is treated classically [31]. This suggests that here too, as in the FDCS for ionization of atomic targets (see above), the interference may be due to the coherent sum of transition amplitudes with and without the PT interaction. In this case the coherence requirement is $\Delta r > \Delta b$ [26], where Δb is the difference in the impact parameter ranges, mostly contributing to a given θ, between the interfering amplitudes. In the measured DCSs for 25 keV $p + H_2$ we do not observe any structures; however, the scattering angles where the extrema occur in R coincide roughly with those predicted by theory for a He target. The ratios measured for He, shown as open symbols in Fig. 5, are very similar to those for H_2. However, the minimum near 0.5 mrad, which is rather weak for H_2 already, is even less pronounced, if present at all.

The solid curve in Fig. 5 represents the ratio between the calculations of Ref. [31] treating the PT interaction quantum-mechanically within the eikonal approximation [dashed curve in Fig. 3(a) of [31]] and classically [dash-dotted curve in Fig. 3(a) of [31]], respectively. For a better comparison with experiment in shape the theoretical ratios were scaled up by 1.35. As far as interference between transition amplitudes with and without this interaction is concerned, these calculations correspond to a coherent and an incoherent treatment. However, it should be noted that there are also differences between the two calculations which are not related to the coherence. The calculation treating the PT interaction classically uses the ansatz [31]

$$d\sigma_{SC}/d\Omega(\theta) = d\sigma_{el}/d\Omega(\theta)\, P_{SC}(\theta), \qquad (4)$$

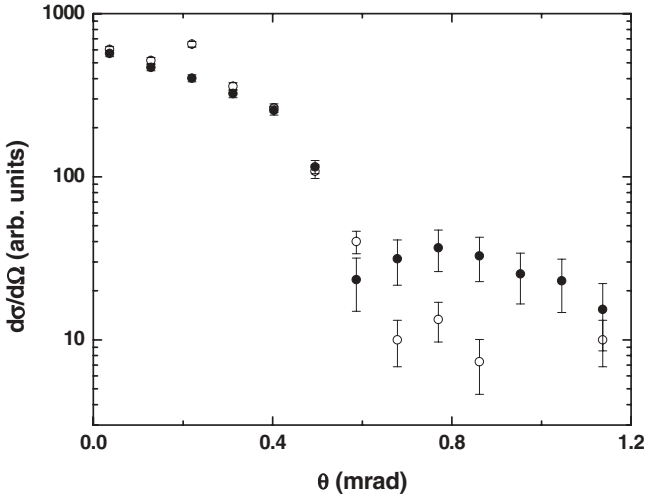

FIG. 6. Same as Fig. 2 for dissociative capture in 25 keV $p + H_2$.

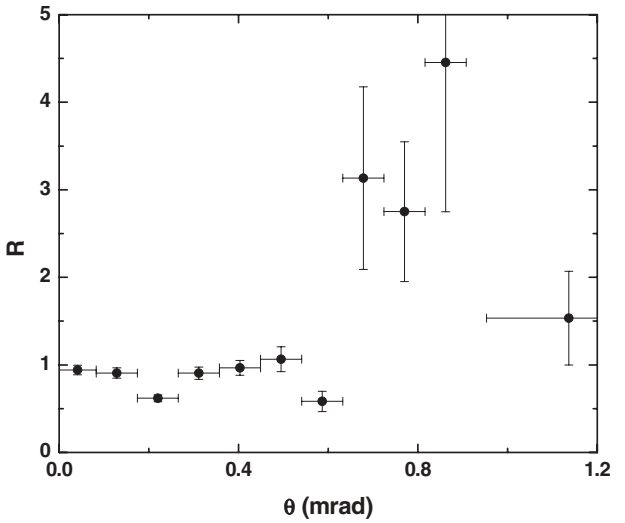

FIG. 7. Same as Fig. 3 for dissociative capture in 25 keV $p + H_2$.

where $d\sigma_{SC}/d\Omega(\theta)$ is the differential capture cross section, $d\sigma_{el}/d\Omega(\theta)$ the elastic scattering cross section, and $P_{SC}(\theta)$ the capture probability. This ansatz is not valid at θ smaller than approximately the inverse projectile momentum ($\approx$0.5 mrad) [33] even if interference between the amplitudes with and without the PT interaction is unimportant. It leads to an unphysically steep increase in the cross sections (compared to both the experimental data and the calculation treating the PT interaction quantum-mechanically) at small θ. There, the interference is not expected to be significant because the deflection of the projectile is dominated by an interaction with the target electron. The comparison between the theoretical and experimental R is thus only meaningful for θ larger than approximately 0.5 mrad. In this angular range the agreement between the calculation and the measured R is surprisingly good, at least qualitatively. This shows that indeed interference effects, not immediately obvious in the absolute DCSs, are actually present. On the other hand, the minimum predicted by theory around 0.7 mrad is much weaker in the experimental data (at least for the He target). This, along with the absence of structures in the measured absolute DCSs, suggests either that the interference is overestimated by theory or that the projectile beam was not fully coherent over the entire angular range even at the large slit distance.

Finally, in Fig. 6 we present DCSs for dissociative capture in 25 keV $p + H_2$ collisions. Here too, the molecular orientation was not determined in the experiment. Overall, the θ dependence of both DCS_{coh} and DCS_{inc} is significantly flatter than in the counterparts for single capture. This is expected because dissociation requires a transition of the second target electron since the ground state of H_2^+ is not dissociative. Otherwise, the comparison between DCS_{coh} and DCS_{inc} is very similar to that for single capture: again, the DCSs are practically identical up to about 0.6 mrad. Unfortunately, at larger θ the statistical fluctuations are considerably larger than for single capture, especially in DCS_{inc}. There, the DCSs are so small that in the range $\theta = 0.9$ to 1.1 mrad incoherent dissociative capture events could not even be detected. Nevertheless, even considering the large error bars, for $\theta > 0.6$ mrad DCS_{coh} is systematically larger than DCS_{inc}. In R, plotted in Fig. 7, this behavior is reflected by a θ dependence which closely resembles the one observed for single capture from He and H_2. In the case of single capture from He and dissociative capture from H_2 the covered θ range is not large enough to determine the location of the maximum, which for single capture from H_2 occurs at 1.2 mrad. But the rising edge appears to be slightly shifted to smaller θ for the He target and further shifted for dissociative capture.

The similarity in the structures between the He and H_2 targets and between single capture and dissociative capture observed in the θ dependence of R suggests that in all cases they result from the same cause. The presence of this structure for an atomic target rules out molecular two-center interference. At the same time in theoretical calculations interference effects are no longer visible if the PT interaction is treated classically [31]. This leads us to conclude that the structures are due to path interference between different impact parameters (depending on the extent to which the PT interaction is responsible for the projectile deflection) leading to the same scattering angle.

IV. CONCLUSIONS

We have measured differential cross sections for single and dissociative capture as a function of scattering angle in collisions of 25 and 75 keV protons with He and H_2. The results confirm our previous conclusion [22] that atomic scattering cross sections can, under certain conditions, depend on the projectile coherence. For 75 keV $p + H_2$ we observe pronounced molecular two-center interference structures in the ratio R between the cross sections for a coherent and an incoherent projectile beam similar to those reported previously for ionization in the same collision system. For 25 keV, in contrast, the structures in R are not mostly due to molecular two-center interference (although it may partly contribute), but rather they are to a large extent due to path interference between different impact parameters leading to the same scattering angle. It cannot be ruled out that the measured R for 75 keV also contain non-negligible contributions from his type of interference. Theory had predicted such structures

[31,32], but in experiment they were so far not observed. Only at very small energy were interference effects found; however, in that case they are due to spatially separated quasimolecular coupling regions [34], i.e., they are of a different nature. The present data show that path interference between different impact parameters is indeed present at larger energies (25 keV). However, it is either significantly weaker than in the calculations or the projectile beam in our experiment was not fully coherent over the entire angular range even at the large slit distance. Furthermore, our results support the conclusion of Wang *et al.* [26] that the widely debated discrepancies between theory and experiment in fully differential cross sections for ionization of helium by fast C^{6+} impact [5] could be caused by such a path interference in the calculations, which does not occur in the experimental data because there the projectile beam was incoherent.

Our studies on the role of the projectile coherence represent an important step towards resolving long-standing puzzling discrepancies between theory and experiment. Here, we discussed two examples regarding fully differential ionization cross sections for fast-ion impact and differential capture cross sections for intermediate-velocity proton impact. Nevertheless, further studies on this topic are called for. Regarding molecular targets, fully differential measurements on ionization are under way. These experiments should reveal coherence effects much more sensitively. Furthermore, we plan to extend the studies on dissociative capture to measure the molecular orientation. By analyzing the ratio between the coherent and incoherent data (i.e., the interference term) as a function of the molecular orientation in principle it is possible to obtain more detailed information about the coherence length. Regarding atomic targets fully differential measurements on ionization for large perturbation parameters are very important. Here, the discrepancies with theory were particularly severe and it is critical to determine whether this can be mostly blamed on the projectile coherence.

The obvious theoretical challenge is to describe an incoherent projectile beam. Presenting the projectile in terms of a wave packet with finite width is probably not feasible at present since it would require an enormous number of angular momentum states. We propose to model the effects of an incoherent beam in a simplified manner using, e.g., the second Born approximation. As discussed in this article the interference term between the first-order amplitude and the second-order amplitude involving the projectile–target nucleus interaction may not be present in the experiment if the projectile beam is incoherent. An easy way to model an incoherent beam would thus be to simply omit the cross term between the two amplitudes.

ACKNOWLEDGMENTS

This research was supported by the National Science Foundation (Grant No. 0969299). G.S. acknowledges support by the Fulbright Foundation. We are grateful for fruitful discussions with many friends and colleagues.

[1] Dz. Belkic, I. Mancev, and J. Hanssen, Rev. Mod. Phys. **80**, 249 (2008).
[2] M. E. Rudd, Y.-K. Kim, D. H. Madison, and J. W. Gallagher, Rev. Mod. Phys. **57**, 965 (1985).
[3] R. Moshammer, P. D. Fainstein, M. Schulz, W. Schmitt, H. Kollmus, R. Mann, S. Hagmann, and J. Ullrich, Phys. Rev. Lett. **83**, 4721 (1999).
[4] R. Moshammer, A. N. Perumal, M. Schulz, V. D. Rodriguez, H. Kollmus, R. Mann, S. Hagmann, and J. Ullrich, Phys. Rev. Lett. **87**, 223201 (2001).
[5] M. Schulz, R. Moshammer, D. Fischer, H. Kollmus, D. H. Madison, S. Jones, and J. Ullrich, Nature (London) **422**, 48 (2003).
[6] A. L. Harris, D. H. Madison, J. L. Peacher, M. Foster, K. Bartschat, and H. P. Saha, Phys. Rev. A **75**, 032718 (2007).
[7] A. B. Voitkiv and B. Najjari, Phys. Rev. A **79**, 022709 (2009).
[8] J. Fiol, S. Otranto, and R. E. Olson, J. Phys. B **39**, L285 (2006).
[9] M. Schulz, M. Dürr, B. Najjari, R. Moshammer, and J. Ullrich, Phys. Rev. A **76**, 032712 (2007).
[10] R. E. Olson and J. Fiol, J. Phys. B **36**, L365 (2003).
[11] F. Jarai-Szabo and L. Nagy, J. Phys. B **40**, 4259 (2007).
[12] J. Colgan, M. S. Pindzola, F. Robicheaux, and M. F. Ciappina, J. Phys. B **44**, 175205 (2011).
[13] M. Dürr, B. Najjari, M. Schulz, A. Dorn, R. Moshammer, A. B. Voitkiv, and J. Ullrich, Phys. Rev. A **75**, 062708 (2007).
[14] D. H. Madison, D. Fischer, M. Foster, M. Schulz, R. Moshammer, S. Jones, and J. Ullrich, Phys. Rev. Lett. **91**, 253201 (2003).
[15] M. McGovern, C. T. Whelan, and H. R. J. Walters, Phys. Rev. A **82**, 032702 (2010).
[16] M. Foster, J. L. Peacher, M. Schulz, D. H. Madison, Zhangjin Chen, and H. R. J. Walters, Phys. Rev. Lett. **97**, 093202 (2006).
[17] A. C. Laforge, K. N. Egodapitiya, J. S. Alexander, A. Hasan, M. F. Ciappina, M. A. Khakoo, and M. Schulz, Phys. Rev. Lett. **103**, 053201 (2009).
[18] R. O. Barrachina and M. Zitnik, J. Phys. B **37**, 3847 (2004).
[19] G. R. Satchler, C. B. Fulmer, R. L. Auble, J. B. Ball, F. E. Bertrand, K. A. Erb, E. E. Gross, and D. C. Hensley, Phys. Lett. B **128**, 147 (1983).
[20] J. K. Swenson, J. Burgdörfer, F. W. Meyer, C. C. Havener, D. C. Gregory, and N. Stolterfoht, Phys. Rev. Lett. **66**, 417 (1991).
[21] J.-Y. Chesnel, A. Hajaji, R. O. Barrachina, and F. Fremont, Phys. Rev. Lett. **98**, 100403 (2007).
[22] K. N. Egodapitiya, S. Sharma, A. Hasan, A. C. Laforge, D. H. Madison, R. Moshammer, and M. Schulz, Phys. Rev. Lett. **106**, 153202 (2011).
[23] C. Keller, J. Schmiedmayer, and A. Zeilinger, Opt. Commun. **179**, 129 (2000).
[24] L. Sarkadi, Phys. Rev. A **82**, 052710 (2010).
[25] X. Y. Ma, X. Li, S. Y. Sun, and X. F. Jia, Europhys. Lett. **98**, 53001 (2012).

[26] X. Wang, K. Schneider, A. LaForge, A. Kelkar, M. Grieser, R. Moshammer, J. Ullrich, M. Schulz, and D. Fischer (submitted to J. Phys. B).
[27] A. D. Gaus, W. Htwe, J. A. Brand, T. J. Gay, and M. Schulz, Rev. Sci. Instrum. **65**, 3739 (1994).
[28] N. Stolterfoht, B. Sulik, V. Hoffmann, B. Skogvall, J. Y. Chesnel, J. Rangama, F. Frèmont, D. Hennecart, A. Cassimi, X. Husson, A. L. Landers, J. A. Tanis, M. E. Galassi, and R. D. Rivarola, Phys. Rev. Lett. **87**, 023201 (2001).
[29] *Atomic Data for Fusion*, edited by C. F. Barnett (Oak Ridge National Laboratory, Oak Ridge, 1990), Vol. 1, p. A-28.
[30] A. Senftleben, T. Pflüger, X. Ren, O. Al-Hagan, B. Najjari, D. Madison, A. Dorn, and J. Ullrich, J. Phys. B **43**, 081002 (2010).
[31] M. Zapukhlyak, T. Kirchner, A. Hasan, B. Tooke, and M. Schulz, Phys. Rev. A **77**, 012720 (2008).
[32] A. L. Harris, J. L. Peacher, and D. H. Madison, Phys. Rev. A **82**, 022714 (2010).
[33] P. T. Greenland, J. Phys. B **14**, 3707 (1981).
[34] L. K. Johnson, R. S. Gao, R. G. Dixson, K. A. Smith, N. F. Lane, R. F. Stebbings, and M. Kimura, Phys. Rev. A **40**, 3626 (1989).